

Supporting Information

for

Preparation of Extracellular Matrix Materials with Antibacterial Activity through Incorporating Biosynthesized ZnO Nanoparticles

Yuqing Han¹, Jie Jiang¹, Jinjin Li^{1*}, Ling Zhao^{1,2} and Zhenhao Xi^{1,2*}

¹ State Key Laboratory of Chemical Reaction Engineering, School of Chemical Engineering, East China University of Science and Technology, Shanghai 200237, China

² Shanghai Key Laboratory of Multiphase Materials Chemical Engineering, East China University of Science and Technology, Shanghai 200237, China

*Corresponding authors:

E-mail (Jinjin Li): lijinjin@ecust.edu.cn

E-mail (Zhenhao Xi): zhxi@ecust.edu.cn

Postal Address: Campus Box 369, No. 130 Meilong Road, Shanghai 200237

Experimental Section

Materials

Sodium dodecyl sulfate (SDS, GC), zinc chloride (ZnCl_2 , Purum $\geq 99\%$), tannin acid (TA, AR), and standard zinc oxide (ZnO) nanoparticles (NPs) were purchased from Macklin Biochemical (Shanghai, China). Collagenase I (BR), elastase (BR), DNase (BR, 300 U/mg), RNase (BR, 60 U/mg), and porcine whole blood were obtained from Yuanye Bio-Technology (Shanghai, China). Triton X-100 (AR) was gained from Titan Scientific (Shanghai, China). PBS was from Beyotime Biotechnology (Shanghai, China). Fresh fish swim bladders (FSBs) were purchased from a local aquatic product market (Shanghai, China) and decellularized through a reported method¹. For this, FSBs were immersed in 1% (w/v) SDS aqueous and 1% w/v Triton X-100 aqueous for 6 h and 0.5 h at room temperature with mild stirring, respectively. After treatment with DNase and RNase solution, the obtained acellular fish swim bladders (AFSBs) were stored at $-20\text{ }^\circ\text{C}$ until further treatment. The bacteria strains of *Escherichia coli* (*E. coli*, ATCC 25922) and *Staphylococcus epidermidis* (*S. epidermidis*, ATCC 12228) were obtained from Microbiological Culture Collection Center (Beijing, China).

Characterization of ZnO-TA NPs

The crystalline structure of NPs was identified through X-ray diffraction (XRD) using a rotating anode X-ray powder diffractometer (D/MAX-2550/PC, Rigaku). Fourier transform infrared spectroscopy (FTIR) spectra were recorded to evaluate the chemical structures and characteristic functional groups of NPs by a spectrometer

(Nicolet is50, Thermo Fisher Scientific). The measurements were operated between 400 to 4000 cm^{-1} with an acquisition of 32 scans. To investigate the nanostructure and size distribution, the NPs were dispersed in ethanol under ultrasonic, dropped on a carbon-coated copper grid, and observed by transmission electron microscopy (TEM, JEM-2100, JEOL), and the images were analyzed by the Image-J software. Additionally, scanning electron microscopy (SEM, JSM-6360LV, JEOL) was utilized to identify the morphology and agglomeration of NPs after sputtering with platinum (Pt). To measure the hydrodynamic sizes and the zeta potential of the nanoparticles, the ZnO NPs and the TA-synthesized ZnO (ZnO-TA) NPs were separately dispersed in deionized (DI) water under supersonic treatment, and each suspension was subjected to a Static and Dynamic Light Scattering Goniometer (CG5-3, ALV). The amount of TA loaded on the ZnO-TA NPs was determined using UV-visible spectrophotometric analysis (UV-1800, Shimadzu) after dissolving the nanoparticles in 5 M hydrochloric acid aqueous solution to a final concentration of 150 $\mu\text{g}/\text{mL}$.

Characterization of NPs-modified AFSBs

Attenuated total reflection fourier infrared (ATR-FTIR) was performed to consider the functional groups of the composite AFSBs using a Nicolet is50 spectrometer (Thermo Fisher Scientific) with a diamond crystal detector. Samples were placed over the diamond crystal and applied standardized pressure to ensure optimal optical contact between the samples and the crystal. ATR-FTIR peaks with scanning frequencies from 4000 to 600 cm^{-1} were used to confirm the functional groups.

SEM equipped with energy-dispersive X-ray spectroscopy (EDS) were utilized to

characterize the distribution of NPs in the AFSBs. Briefly, the freeze-dried samples were quenched in liquid nitrogen to obtain fracture surfaces and the scanned surfaces were sputter-coated with Pt for 60 s at 30 mA before scanning. All samples were examined using an accelerating voltage of 3 kV.

The hydrophilicity of AFSBs was determined by the water contact angle (WCA) analysis at room temperature through a goniometer (JC2000A, Shanghai Zhongcheng Digital Equipment Co.). In brief, the samples were mounted on a microscope slide with double-sided adhesive tape and dropped with 2 μ L deionized (DI) water on their surfaces. The contact angle between the water droplet and the surface of the sample was measured.

Antibacterial activity of NPs

The antibacterial activity of nanoparticles was assessed by the optical density (OD) method. In brief, ZnO NPs and ZnO-TA NPs were dispersed in Luria-Bertani (LB) broth at concentrations of 0, 10, 25, 50, 100, 200, and 400 μ g/mL, respectively. The *E. coli* and *S. epidermidis* cultures were added to the LB broth containing nanoparticles, achieving a final concentration of 10^7 CFU/mL. The mixtures were incubated at 37 $^{\circ}$ C and the absorbances were measured at 600 nm each hour to monitor bacterial growth. The LB broth containing different concentrations of NPs without bacteria was performed as blank, and the LB broth containing bacteria was performed as control. The inhibition efficiency was calculated by the following equation:

$$\text{Inhibition efficiency (\%)} = (\text{OD}_c - \text{OD}_s) / \text{OD}_c \times 100\%$$

Where the OD_c represents the OD values of the LB broth containing bacteria without

nanoparticles, and the OD_s is the OD values of the LB broth containing bacteria and nanoparticles.

Results and Discussion

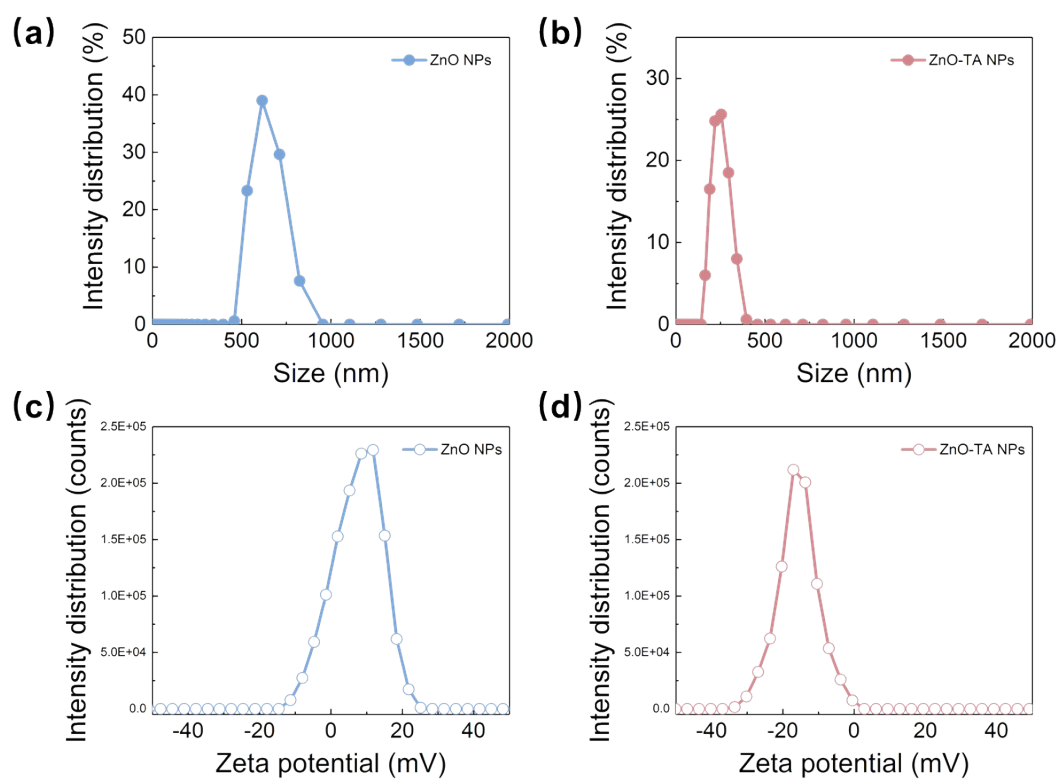


Fig. S1. The hydrodynamic size distribution of (a) ZnO NPs and (b) ZnO-TA NPs, and the zeta potential distribution of (c) ZnO NPs and (d) ZnO-TA NPs.

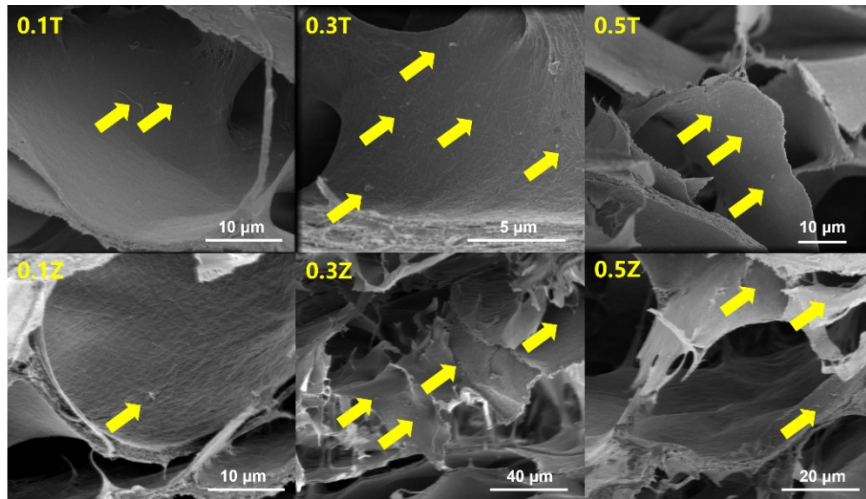


Fig. S2. SEM photographs of NPs-modified AFSBs sections.

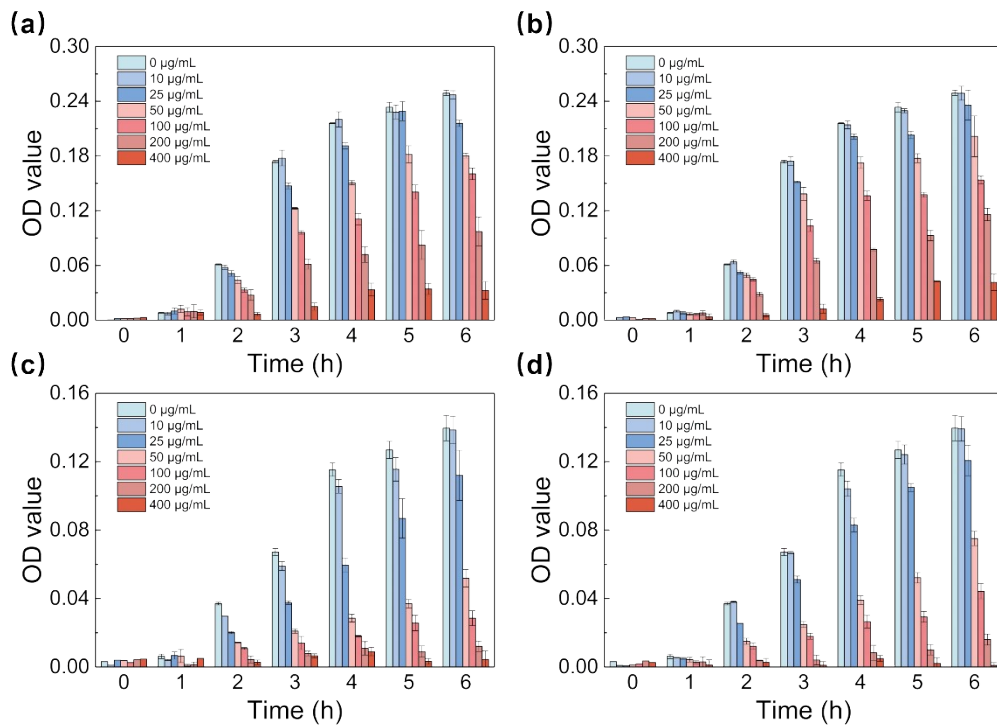


Fig. S3. Antibacterial activity of (a) ZnO NPs and (b) ZnO-TA NPs against *E. coli* and antibacterial activity of (c) ZnO NPs and (d) ZnO-TA NPs against *S. epidermidis*. (*: $p < 0.05$)

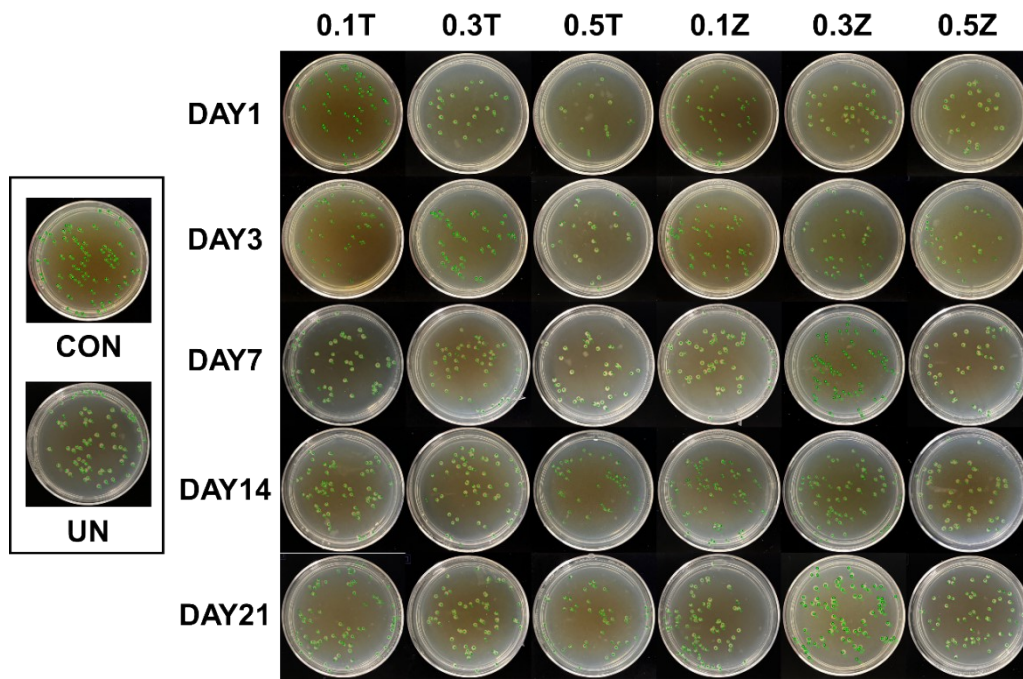


Fig. S4. The images of *E. coli* plates. (Dilution factor was 10^6)

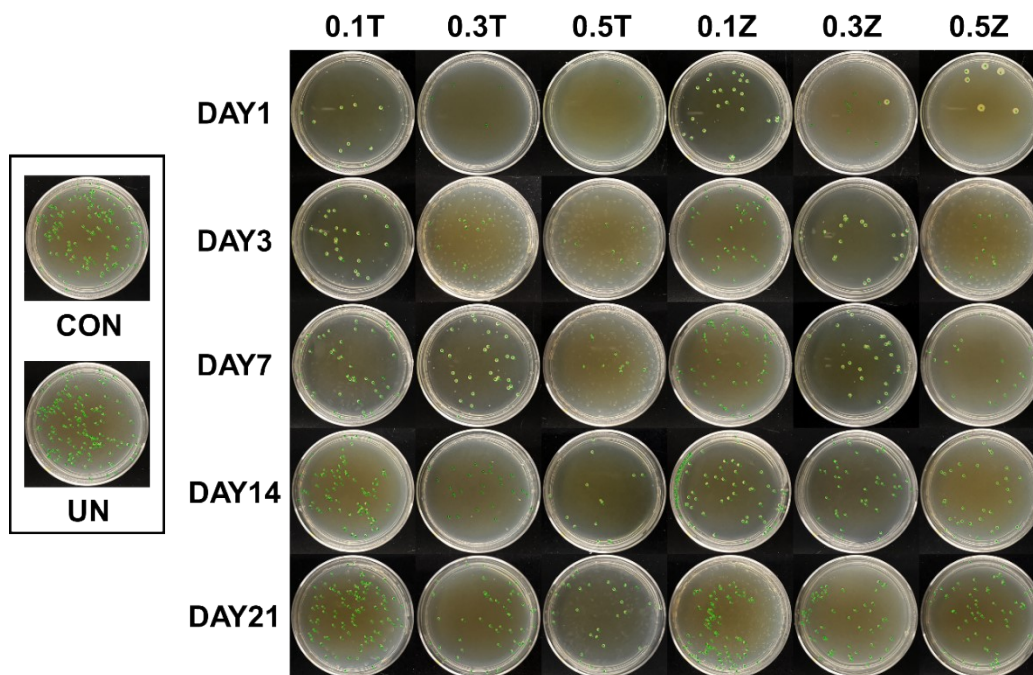


Fig. S5. The images of *S. epidermidis* plates. (Dilution factor was 10^6)

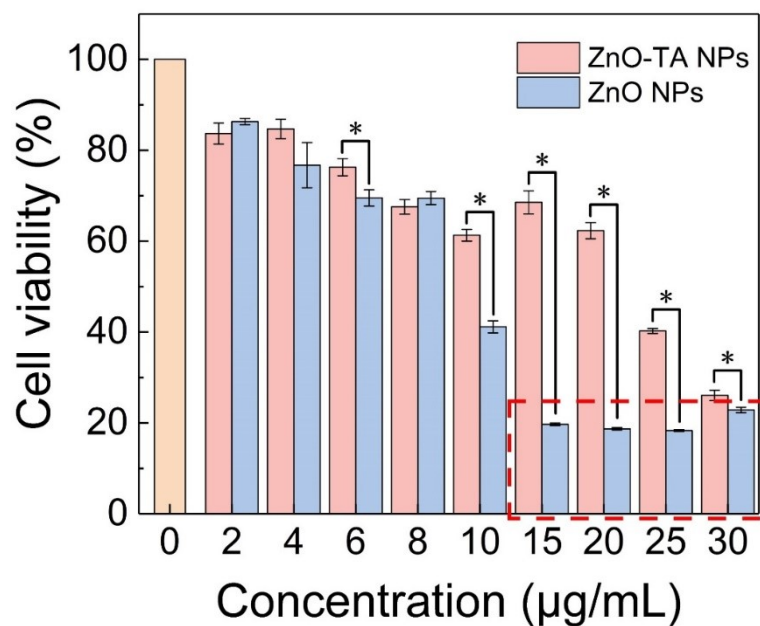


Fig. S6. Cell viability of L929 cells incubated with ZnO-TA NPs and ZnO NPs. (*: $p < 0.05$)

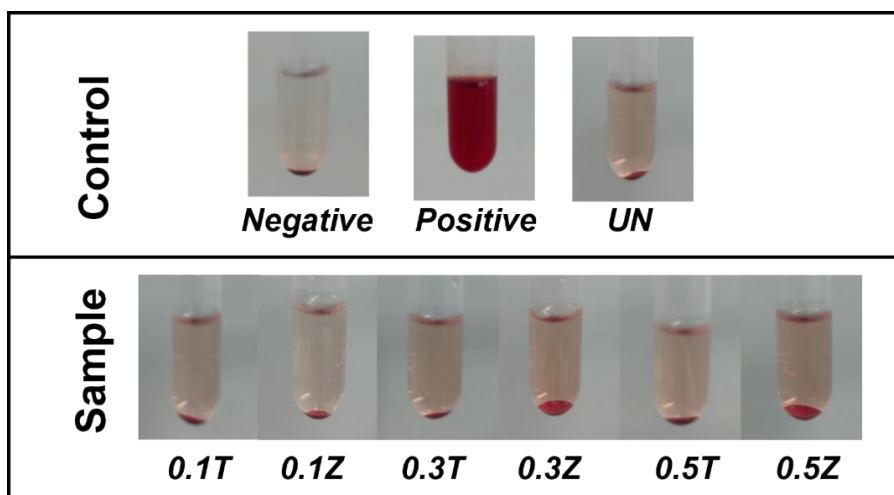


Fig. S7. Hemolysis images of NPs-modified AFSBs.

Table S1. The number of colonies on *E. coli* plates.

Colony counts ($10^7/mL$)	0.1T	0.3T	0.5T	0.1Z	0.3Z	0.5Z
	15	2	0	26	8	2

1	35	27	16	47	33	26
3	39	32	25	52	34	27
7	51	47	36	58	52	39
14	66	53	43	66	67	50
21	77	56	51	81	73	57

Where the colony count is 75 ($10^7/\text{mL}$) and 67 ($10^7/\text{mL}$) of the UN and control, respectively.

Table S2. The number of colonies on *S. epidermidis* plates.

Colony counts ($10^7/\text{mL}$)	0.1T	0.3T	0.5T	0.1Z	0.3Z	0.5Z
0	4.6	3.4	1.9	7	6	3.4
1	10	4	2	25	9	6
3	26	12	8	38	19	12
7	45	27	10	49	24	19
14	78	26	14	81	41	33
21	98	50	28	96	59	60

Where the colony count is 164 ($10^7/\text{mL}$) and 124 ($10^7/\text{mL}$) of the UN and control, respectively.

Reference

1. J. Liu, B. Li, H. Jing, Y. Wu, D. Kong, X. Leng and Z. Wang, *Adv. Healthc. Mater.*, 2020, **9**, 1901154.